PAPER

Nanostructured polymer brushes and protein density gradients on diamond by carbon templating†

Naima A. Hutter,[a] **Marin Steenackers,**[ac] **Andreas Reitinger,**[b] **Oliver A. Williams,**[d] **Jose A. Garrido**[*b] **and Rainer Jordan**[*ae]

Micro- and nanostructured polymer brushes on diamond can be directly prepared by carbon templating and amplification of the latent structures by photografting of a broad variety of vinyl monomers such as styrenes, acrylates and methacrylates. Even template structures with lateral dimensions as small as 5 nm can be selectively amplified and defined polymer brush gradients of a variety of functional polymers are realizable by this technique. Furthermore, conjugation with a model protein (GFP) results in protein density gradients of high loading and improved chemical stability. The effective functionalization of chemically and biologically inert diamond surfaces with stable functional polymer brushes, the possibility of structuring by the carbon templating technique and the direct biofunctionalization are crucial steps for the development of diamond based biosensors.

1. Introduction

The functional integration of soft biological entities and hard semiconductor systems is crucial for the development of biosensors and the incorporation of microelectronic systems within living organisms.[1,2] Due to the poor biocompatibility and chemical stability of silicon-based materials, alternative substrate material is one focus of the current research. Especially conductive diamond thin films combine chemical stability and bioinertness, as well as a large electrochemical potential window and a small background current as electrode material in aqueous media.[3–5] In the perspective of using diamond for biomedical applications, there have been numerous approaches to the immobilization of biomolecules on diamond thin films.[3,5–7] While previous studies on the biofunctionalization of diamond focused on the formation of monolayers, it has been shown that polymer brushes are ideal systems to tailor soft interfaces in order to combine biological systems and rigid substrates.[8,9]

The development of diamond-based biosensors for high-throughput and parallel screening requires versatile patterning methods. Recently, we have reported on the carbon-templating (CT) technique which allows the fabrication of structured polymer brushes on substrates, independent of the surface chemistry and with near-molecular precision.[10]

Here, we report on the nanostructuring of hydrogenated nanocrystalline diamond (NCD) thin films by CT. Template structures of line widths from 2 μm down to 5 nm were successfully amplified by the polymerization of vinyl monomers. Furthermore, we demonstrate two chemical approaches for the direct preparation of protein density gradients with a high loading capacity by the conjugation of brush structures with the green fluorescent protein (GFP).

2. Results and discussion

The preparation of structured polymer brushes on conductive boron doped NCD is outlined in Fig. 1. AFM measurements confirm the selective formation of polymer brushes on the carbon
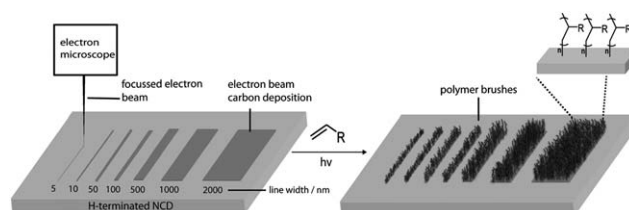
a Wacker-Lehrstuhl für Makromolekulare Chemie, Department Chemie, Technische Universität München, Lichtenbergstraße 4, 85747 Garching, Germany. E-mail: Rainer.Jordan@tu-dresden.de
b Walter Schottky Institut, Technische Universität München, Am Coulombwall 3, 85748 Garching, Germany. E-mail: Garrido@wsi.tum.de
c Institute for Advanced Study, Technische Universität München, Arcisstraße 21, 80333 München, Germany
d Fraunhofer Institute for Applied Solid State Physics, Tullastraße 72, 79108 Freiburg, Germany
e Professur für Makromolekulare Chemie, Department Chemie, TU Dresden, Zellescher Weg 19, 01069 Dresden, Germany
† Electronic supplementary information (ESI) available. See DOI: 10.1039/c1sm05082f

Fig. 1 Preparation of structured polymer brushes on diamond. On the native NCD surface structures of electron beam-induced carbon deposits are created by means of a focussed electron beam. The 10 μm long CT lines had widths of 2 μm, 1 μm, 500 nm, 100 nm, 50 nm, 10 nm and 5 nm. The carbon templates were amplified by the SIPGP to structured polymer brushes.

templates *via* the UV-induced self-initiated photografting and photopolymerization (SIPGP) mechanism of a broad variety of vinyl monomers (detailed scheme of the reaction mechanism can be followed in ESI1†).[11,12] The selectivity of the photografting is due to the different bond dissociation energies (BDEs) of hydrogenated NCD (BDE of C–H: 401.5 kJ mol^{-1}) and of the carbon templates (BDE between 84 and 301 kJ mol^{-1}).[10,13]

To investigate the smallest template structure size that can be amplified by SIPGP, seven 10 μm long CT lines of decreasing width (2 μm to 5 nm) were prepared (Fig. 1). In Fig. 2 the selectivity of the photografting process for 2-isopropenyl-2-oxazoline (IPOx) is shown. The amplification of the structures by SIPGP of IPOx could be unambiguously detected by AFM for the line widths of 2 μm, 1 μm, 500 nm, 100 nm to 50 nm, whereas narrower lines (10 nm and 5 nm) could not be resolved (Fig. 2) because of the substrate roughness. However, after a second grafting by living cationic ring-opening polymerization (LCROP) of 2-ethyl-2-oxazoline (EtOx), resulting in bottle-brush brushes (BBB),[14–16] larger polymer brush structures on latent carbon templates of projected line widths down to 5 nm could be unambiguously identified because of the structure amplification. This is in agreement with recent studies which have shown that the height and width of nanostructured polymer brushes correlate with the footprint structure size due to the extension of the grafted chains to the polymer-free surface regions, also resulting in a broadening of the structures (Fig. 2).[17–20]

The CT-approach provides a direct tool to control not only the 2D locus of the grafting points for the SIPGP reaction as demonstrated in Fig. 1 and 2 but also, by varying the locally applied electron dose, the polymer grafting density as shown in the series of gradients displayed in Fig. 3.[10] The gradient structures were prepared by linearly increasing the electron doses during lithography from 0 to 100 mC cm^{-2} over a range of 50 μm^2. In a series of experiments, styrene, 2-isopropenyl-2-oxazoline (IPOx), 4-vinyl pyridine as well as different acrylates such as methylmethacrylate (MMA), *tert*-butyl methacrylate (*t*BuMA), and *N,N*-dimethyl-aminoethyl methacrylate (dMAEMA) were grafted onto 10×50 μm^2 gradient CTs by means of SIPGP. It can be observed that the profile of the polymer brush height reaches a maximum level at approx. 40 mC cm^{-2} independent of the type of polymer. The correlation between the polymer thickness and electron dose used for the templating step can be explained by an increase of the polymer grafting density at higher e-beam doses.[10] Besides the UV irradiation time in the bulk monomer, the electron dose thus provides an additional tool in order to control the polymer layer thickness.[14]

The thermal and chemical stability of the polymer brush structures is a crucial issue for various applications *i.e.* for the long time use of biosensors in complex biological systems. AFM measurements on different gradients shown in Fig. 3 revealed that neither extraction with boiling toluene for 3 h, treatment with diluted sulfuric- and nitric acid nor elevated temperatures
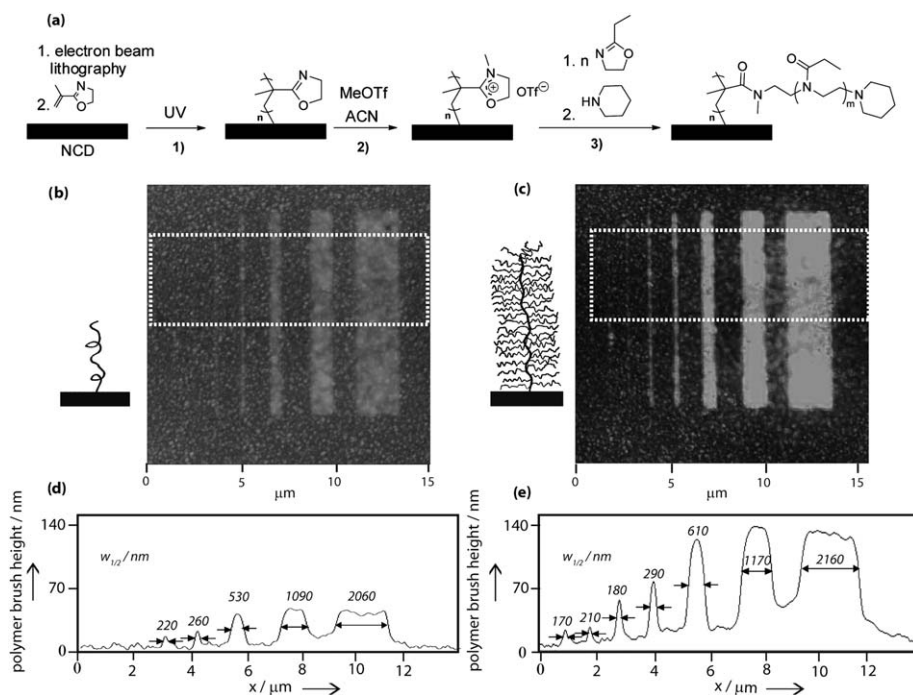

Fig. 2 Preparation of structured P(IPOx) polymer brushes and P(IPOx-*g*-EtOx) bottle-brush brushes (BBBs) on NCD by the carbon templating technique (carbon template structures of seven lines with increasing line width from 5 nm to 2 μm as shown in Fig. 1). (a) Reaction scheme for the preparation of structured poly(2-oxazoline) BBBs on NCD. (1) SIPGP of IPOx to P(IPOx) brushes. (2) Preparation of the brush macroinitiator PIPOx$^+$OTf$^-$. (3) LCROP of EtOx on macroinitiator brush and termination reaction with piperidine to P(IPOx-*g*-EtOx). (b) AFM of structured P(IPOx) brushes on NCD. (c) AFM of structured P(IPOx-*g*-EtOx) bottle-brush brushes. (d) AFM section analysis of P(IPOx) brushes averaged at the indicated area along with the structure line widths at half height ($w_{1/2}$) after surface polymerization. (e) AFM section analysis of the structured P(IPOx-*g*-EtOx) bottle-brush brushes averaged within the indicated area and $w_{1/2}$.
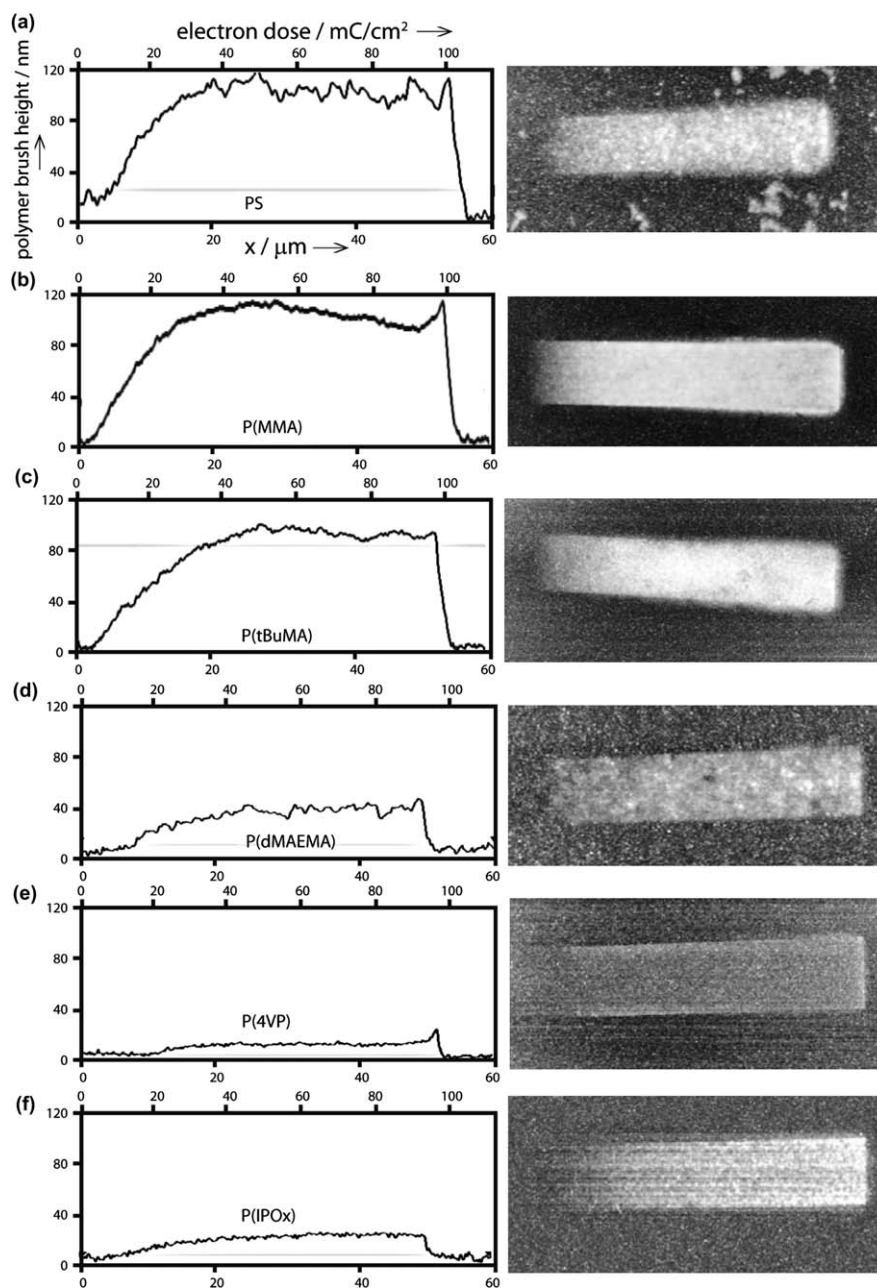
Fig. 3 AFM scans and section analysis of 10×50 μm² polymer brush gradients prepared by the CT technique (linearly increasing electron doses from 0 to 100 mC cm⁻²) and subsequent SIPGP of the following monomers after different UV-irradiation times (t_{SIPGP}) as indicated: styrene (PS, t_{SIPGP}: 24 h), methylmethacrylate (PMMA, t_{SIPGP}: 6 h), *tert*-butyl methacrylate (P*t*BuMA, t_{SIPGP}: 6 h), *N,N*-dimethyl-aminoethyl methacrylate (PdMAEMA, t_{SIPGP}: 2 h), 4-vinyl pyridine (P4VP, t_{SIPGP}: 24 h) and 2-isopropenyl-2-oxazoline (PIPOx, t_{SIPGP}: 24 h).

(4 h at 130 °C in air) led to the desorption of the polymer brushes. However, it was found that the polymer brush structures as well as the carbon deposits could be removed completely in oxygen plasma, allowing the recycling of NCD substrates.

To develop the NCD–polymer brush system for biosensor applications, we first investigated the immobilization of GFP on poly(methacrylic acid) (P(MA)) brushes (Fig. 4) before advancing to more complex polymer architectures such as BBBs (Fig. 5a). A polymer brush gradient as introduced in Fig. 3 is a convenient approach to analyze in a single experiment the conjugation of

bulky biomolecules within polymer brushes of different thicknesses and grafting densities. We prepared a 10×50 μm² brush gradient of poly(*tert*-butyl methacrylate) (P(*t*BuMA)) by CT and SIPGP of *t*BuMA. Hydrolysis under acidic conditions gave P(MA) brushes onto which GFP was coupled to result in polymer brush protein conjugates (Fig. 4a).

The brush gradient profiles as measured by AFM as well as the thickness decrease of 57% after hydrolysis are in good agreement with results obtained previously on Si surfaces (Fig. 4b and c).[10,21] After GFP coupling AFM height profile analysis reveals
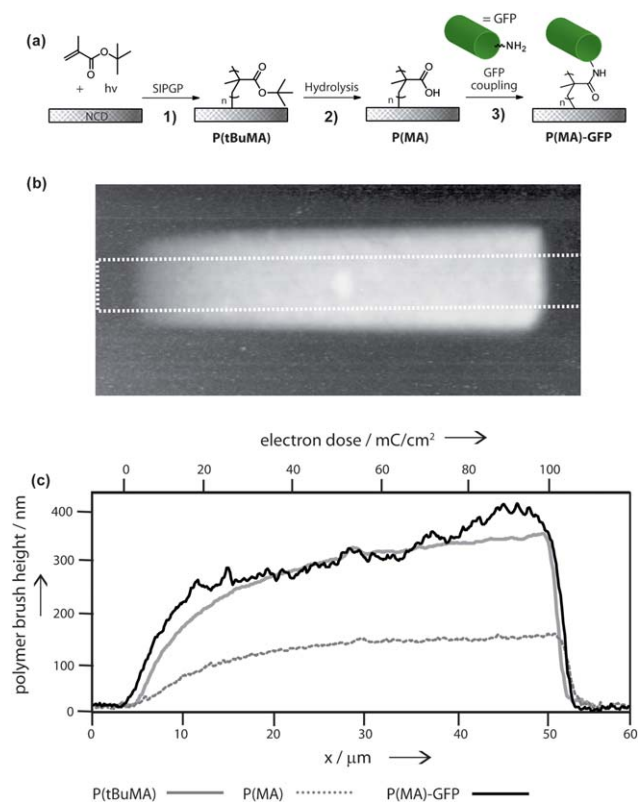
Fig. 4 (a) Preparation of biofunctionalized poly(methacrylic acid) (P(MA)) brushes on NCD. (1) SIPGP of *tert*-butyl-methacrylate resulting in poly(*tert*-butyl-methacrylate) polymer brushes. Hydrolysis to P(MA) (2) and coupling of GFP (3) result in GFP–brush conjugates. (b) AFM of a 10 × 50 μm² P(*t*BuMA) gradient (prepared by CT with a linearly increasing electron dose from 0 to 100 mC cm⁻²). (c) AFM section analysis of the P(*t*BuMA) (grey, averaged at the indicated area), P(MA) (grey dotted) and P(MA)–GFP (black) gradients.

a thickness increase of the gradient at 100 mC cm⁻² from 150 ± 10 nm to 420 ± 30 nm after the protein immobilization step (Fig. 4c). Although a quantitative determination of the protein loading (Ø$_{GFP}$: 2.4 nm; length$_{GFP}$: 4.2 nm)[22] cannot be performed based on these measurements, the remarkable thickness increase can only be explained by multiple protein conjugation to the surface bonded polymer.

Inverted fluorescence microscopy measurements of the intensively cleaned biofunctionalized polymer brushes revealed a strong green fluorescence signal exclusively at the P(MA) modified areas for excitation wavelengths at both 395 and 475 nm,[23] showing the selective covalent immobilization of GFP (Fig. 6b). It should be noted that polyelectrolyte brushes such as P(MA) can strongly adsorb proteins by ionic interactions at high loading capacities. Since the isoelectric point of GFP and the pK_a value for P(MA) are both around 5, it is not possible that the protein immobilization at pH 7.5 is due to ionic interactions. However, to verify this point, ion exchange experiments with different electrolyte solutions were performed and the functionalized substrate exposed to different pH. AFM analysis of the biofunctionalized NCD did not reveal a significant thickness decrease and corroborates a covalent coupling between GFP and P(MA).

Since partially denatured GFP loses its characteristic photophysical properties, the detection of fluorescence is a clear indication for the presence of native GFP coupled to the polymer brush.[24,25] Moreover, despite treatment of the sample under basic conditions that causes denaturation of free GFP[26] and loss of fluorescence, the brush conjugated GFP still shows significant fluorescence, indicating an improved stability of polymer-bonded GFP. The freshly biofunctionalized PMA brush gradient on NCD revealed a strong fluorescence as shown in Fig. 6. After treatment with 0.1 M NaOH overnight (16 h), the fluorescence signal drastically decreases, although a clear contrast between the non-modified and the GFP-functionalized NCD persists. Even after treatment of the PMA–GFP brush with 1 M NaOH overnight (16 h), fluorescence remains detectable (see ESI2†). This improved stabilization of proteins by polymer brush conjugation is an interesting property for the development of stable biosensors.

As P(MA) is a widely applied polymer for the immobilization of biomolecules and the coupling of GFP was successfully demonstrated here, higher structural complexity will allow further control of interfacial properties. Thus, the successful straightforward approach was extended using so-called bottle-brush brushes (BBBs). These molecular structures have gained interest in the design of functional polymers with tailor-made architectures. As they are related to the structure of glycosylated macromolecules located on nearly every living cell,[27,28] bottle-brush polymers have a widened potential due to their biomimetic structure design. Since it has been shown that poly(2-oxazoline)s are non-toxic and that proteins as well as drugs can be coupled to the polymer without losing their activity[29,30] POx-based BBBs appear to be an expedient choice as an immobilization matrix for biomolecules at interfaces.

A polymer brush gradient of P(IPOx) was prepared by CT and SIPGP of IPOx analogue to the experiments using linear polymer brushes with P(MA). The conversion to BBBs was performed as described in Fig. 2a. In order to obtain biofunctional BBBs, the cationic graft polymerization was terminated with a glycine derivative as the bifunctional coupling group to introduce carboxylic acid moieties for the ligation reaction with GFP (see Fig. 5a). The possibility to systematically introduce functional end groups to surface grafted POx bottle-brushes has previously been demonstrated by reacting amine end groups with rhodamine B isothiocyanate and by analyzing the resulting fluorescence.[14] To give an additional proof of principle for the reliability of the termination reaction, X-ray photoelectron spectroscopy (XPS) of differently terminated BBBs on NCD was measured (see ESI3†).

In Fig. 5c the resulting gradient profiles for the different reaction stages as determined by AFM are shown (PIPOx brush, gylcine-*tert*-butylester terminated P(IPOx-*g*-EtOx) and P(IPOX-*g*-EtOx)–GFP). After the LCROP the significant increase of the polymer layer thickness of around 100% from 44 ± 10 nm (at maximum point) to 90 ± 8 nm can be observed which is expected for a successful surface-initiated living cationic polymerization reaction (SI-LCROP) of EtOx. This is in agreement with recent results on micropatterned surfaces using the same SI-LCROP reaction.[16] After end group hydrolysis and GFP coupling, the gradient profile further increases significantly by about 100% to 230 ± 20 nm (at maximum point) because of the increase of the polymer ligand molar mass. This is a good indication for a high
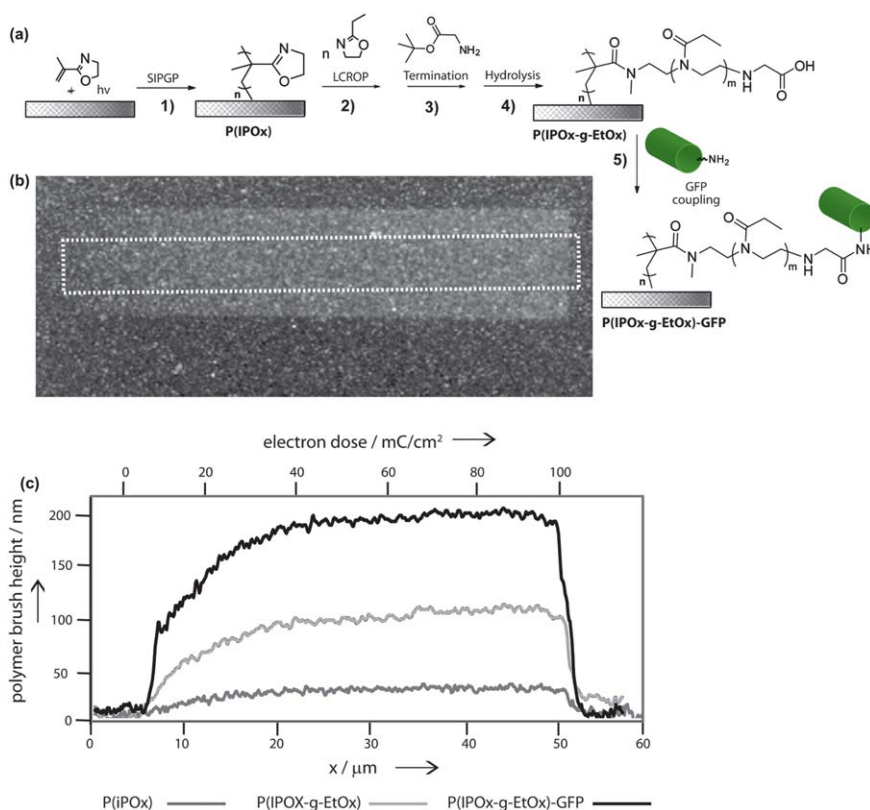
Fig. 5 (a) Preparation of biofunctionalized poly(IPOx-g-EtOx) BBBs on NCD. (1) SIPGP of 2-isopropenyl-2-oxazoline resulting in poly(2-isopropenyl-2-oxazoline) (PIPOx) polymer brushes. LCROP of EtOx according to the procedure described in Fig. 3 (2) and termination reaction with glycine-*tert*-butylester (3) to P(IPOx-g-EtOx). (4) Hydrolysis of the functional end groups to form carboxylic acid functions and subsequent coupling of GFP (5) results in GFP–BBB conjugates. (b) AFM of a 10×50 μm² P(IPOX) gradient (prepared by CT with a linearly increasing electron dose from 0 to 100 mC cm⁻²). (c) AFM section analysis of the P(IPOX) (dark grey, averaged at the indicated area), glycine-*tert*-butylester terminated P(IPOx-g-EtOx) (light grey) and P(IPOx-g-EtOx)-GFP (black) gradients.

GFP functionalization of the polymer BBBs. To verify the bioactivity of the protein being in the native (functional) state, fluorescence microscopy of the P(IPOX-g-EtOx)–GFP gradient was measured. The strong fluorescence of the GFP-functionalized BBBs at the expected wavelength, analogous to the P(MA)–GFP modified sample (Fig. 6e), shows that the GFP was bonded in its active form.

In Fig. 6c and f, the polymer brush gradient height profiles and fluorescence intensities of both the biofunctionalized P(MA) gradient and the P(IPOx-g-EtOx) gradient are compared. The significant increase of the thickness along the entire gradient and the similarity of the height profile and the fluorescence intensity profile indicate that the proteins are immobilized throughout the entire P(MA) brush.[10] If GFP were only coupled within the upmost brush region, the resulting fluorescence intensity would be independent of the polymer layer thickness. Moreover, the gradual increase of the fluorescence intensity correlates with the polymer thickness gradient and shows that the amount of immobilized GFP follows the locally applied electron dose used for the CT step. In other words, CT can be used as a direct tool for the preparation of precise surface patterns on the micrometre down to the nanometre scale as well as for the fabrication of complex biomolecule density gradients. Both aspects, patterning and density gradients, are crucial for the development of

bioresponsive surfaces for sensing as well as for the study of cell surface interactions.

3. Conclusions

The preparation of stable nanostructured polymer brushes on NCD by the carbon templating technique is presented. Carbon templates prepared by EBCD with dimensions down to 5 nm can be selectively amplified into larger polymer structures by SIPGP. The CT technique allows the design of array systems on the micro- and nanometre range with a free choice of possible patterns without the need of a specific surface chemistry, mask, resist or other primary coating. Furthermore, the functionalization of structured P(MA) layers with functional GFP shows that direct immobilization of biomolecules can be achieved on NCD using a polymer brush approach and high biomolecule loading can be realized. Multiple coupling of GFP onto polymer brushes of higher, bioinspired complex architectures (bottle-brush brushes, BBBs) was successfully demonstrated by preparing end group functionalized poly(2-oxazoline) based bottle-brush brushes as soft interlayer on the NCD. Protein density gradients could readily be realized, adding a third tunable variable to the biofunctionalization process of surfaces. The creation of such three-dimensional structures on the nanometre scale is a unique
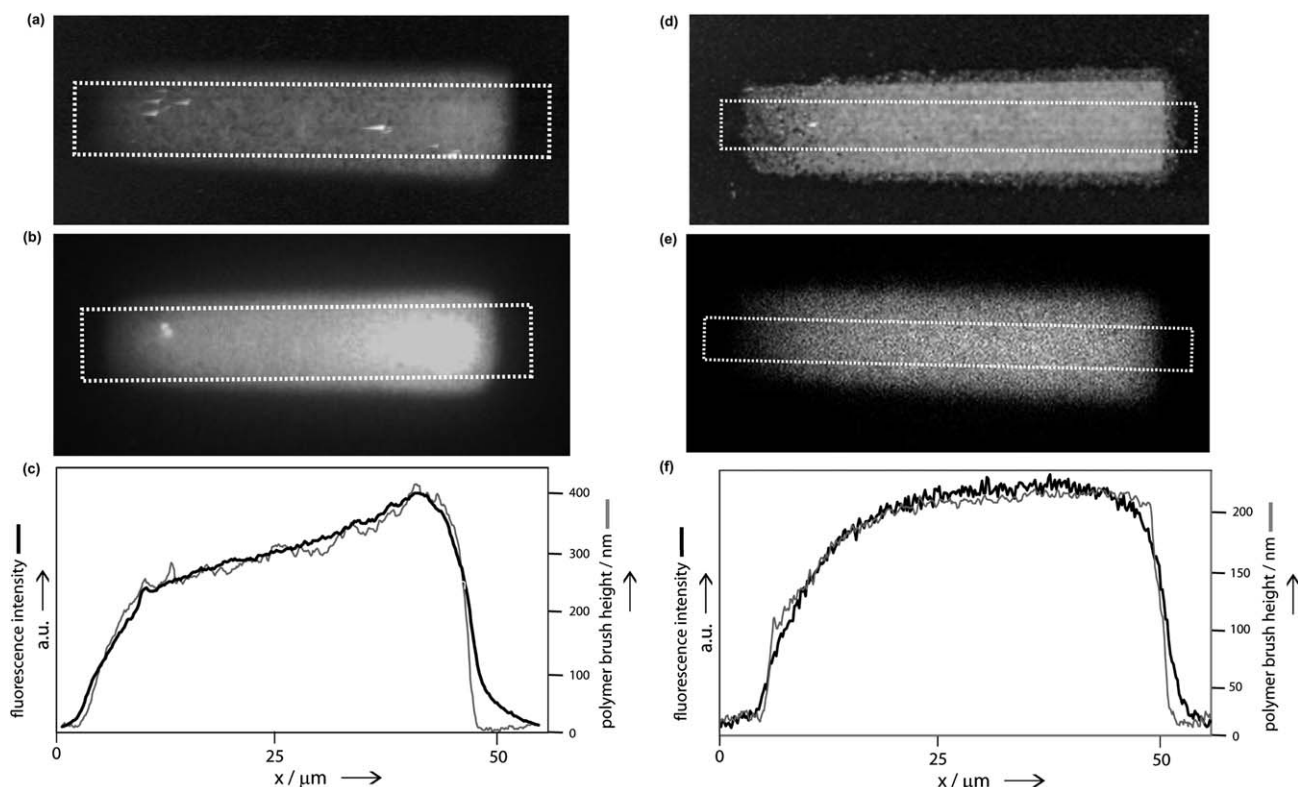
Fig. 6 Analysis of 10 × 50 μm² gradients of P(MA)–GFP and P(IPOx-g-EtOx)–GFP on NCD. (a) AFM scan and (b) fluorescence image of P(MA)–GFP. (c) Normalized profile plot of the fluorescence intensity and of the polymer brush height of the P(MA)–GFP gradient obtained from AFM section analysis (averaged at the indicated area). (d) AFM scan and (e) fluorescence image of P(IPOx-g-EtOx)–GFP. (f) Normalized profile plot of the fluorescence intensity and of the polymer brush height of the P(IPOx-g-EtOx)–GFP gradient obtained from AFM section analysis.

feature of the carbon templating approach. The combination of the presented route for the (bio)functionalization of diamond and a broad variety of possible 2D and 3D designs will enable the study of cell surface interaction with the precise variation of the surface topography, polymer layer mechanics, local biomolecule concentration and its accessibility. These factors are crucial for the realization of complex biosensor arrays for high-throughput screening.

4. Experimental section

Nanocrystalline diamond (NCD) substrates

Metallically doped prime grade silicon {100} wafers were cleaned using standard RCA SC-1 processes ($NH_3OH : H_2O_2 : DI\ H_2O$, 1 : 1 : 5, 75 °C, 10 min). Following a rinsing process of DI H_2O in an ultrasonic bath, wafers were immersed in a colloid of monodisperse diamond nanoparticles, and agitated in an ultrasonic bath for 30 min. Wafers were subsequently rinsed in pure DI H_2O and spun dry under N_2 flow. This process is known to produce nucleation densities in excess of 10^{11} cm^{-2}.[31] Nanocrystalline diamond films were grown on these treated substrates by microwave plasma enhanced chemical vapor deposition at 55 mbar and 3500 watts. The gas phase was 4% methane diluted in hydrogen. A boron/carbon ratio of 6500 ppm was maintained by the addition of trimethylboron gas. Films were grown to 250 nm in thickness, resulting in a surface roughness of 10 nm rms (measured on 5 × 5 μm²).[32] Clean NCD surfaces were

hydrogenated in a microwave plasma setup (100 sccm hydrogen flow, 50 mbar hydrogen pressure, 750 W microwave power, 700 °C sample temperature, for 15 min).

Electron beam induced carbon deposition (EBCD)

Electron beam induced carbon deposition (EBCD) was performed on freshly hydrogenated NCD with a focused electron beam in a Zeiss E-Line scanning electron microscope (vacuum pressure around 2×10^{-5} mbar). The electron beam was run at 20 keV with a beam current of around 300 pA. All structures except gradients were irradiated with an electron dose of 50 mC cm^{-2}. The gradients were prepared with an electron dose linearly increasing from 0 to 100 mC cm^{-2}. It is noteworthy that since the thickness of the carbon deposits lies far beyond the roughness of native NCD (approx. 10 nm rms), we were unable to visualize the carbon templates by AFM measurements before the photopolymerization step.

Self-initiated photografting and photopolymerization (SIPGP)

Freshly prepared NCD substrates structured by EBCD were submerged in approximately 1 mL of distilled and degassed monomer in a photoreaction tube under dry argon atmosphere. Polymerization was carried out under constant irradiation with UV light (300–400 nm; $\lambda_{max} = 350$ nm) at RT. After SIPGP, the samples were immediately cleaned by sequential ultrasonication with different solvents (all HPLC grade) for 5 minutes each.

Solvent series used for cleaning of grafted PS: toluene, ethyl acetate and ethanol; P(MMA): chloroform, ethyl acetate and ethanol; P(tBuMA): dichloromethane, ethyl acetate and ethanol; P(dMAEMA): water, ethanol and ethyl acetate; P(4VP): ethanol, acetonitrile, ethyl acetate and for P(IPOx): chloroform, acetonitrile and ethanol.

Living cationic ring-opening polymerization (LCROP)

The formation of P(IPOx-g-EtOx) bottle-brush brushes was performed as previously reported.[15] As terminating agent, glycine-tert-butylester was added to the polymerization solution to introduce the carboxylic acid moieties to the polymer side chain ends.

GFP labeled polymer brushes and bottle-brush brushes

Both poly(tert-butyl methacrylate) brushes and poly(IPOx-g-EtOx) BBBs terminated with glycine-tert-butylester on NCD were hydrolyzed in a solution of methanesulfonic acid in dichloromethane (1 : 100) at RT for 30 minutes. After ultrasonication in DCM, water and ethanol the samples were immersed in an aqueous solution of 400 mM 1-ethyl-3-(3-dimethylaminopropyl)carbodiimide (EDC) and 100 mM N-hydroxy succinimide (NHS) for 1 hour. After cleaning with buffer solution (phosphate buffer 40 mM) the samples were covered with a solution of GFP in buffer (1.5 mg mL^{-1}) for 24 hours, rinsed thoroughly and stored at 4 °C in buffer solution (phosphate buffer pH 7.5).

In order to verify the covalent character of the bonding between poly(methacrylic acid) brushes and GFP, the biofunctionalized NCD sample was emerged successively in a solution with pH 6, pH 2 and in a strong electrolyte (0.5 M NaCl) for one hour each.

Atomic force microscopy (AFM)

Atomic Force Microscopy (AFM) scans were obtained with a Nanoscope IIIa scanning probe microscope from Veeco Instruments using standard tips in tapping mode (driving amplitude of ~1.25 V at a scan rate of 0.5 Hz). The gradient profiles were obtained by the average section analysis.

Fluorescence microscopy

Fluorescence Microscopy images were obtained with a Zeiss Axiovert 200M MAT microscope equipped with a Hamamatsu Photonics CCD camera and suitable filter sets. The cross-section analysis was performed by pixel analysis of the 256 bit black and white fluorescence image using the Image J software package.

Acknowledgements

References

1 S. Vaddiraju, I. Tomazos, D. J. Burgess, F. C. Jain and F. Papadimitrakopoulos, *Biosens. Bioelectron.*, 2010, **25**, 1553.
2 G. S. Wilson and R. Gifford, *Biosens. Bioelectron.*, 2005, **20**, 2388.
3 A. Härtl, E. Schmich, J. A. Garrido, J. Hernando, S. C. R. Catharino, S. Walter, P. Feulner, A. Kromka, D. Steinmuller and M. Stutzmann, *Nat. Mater.*, 2004, **3**, 736.
4 J. Rubio-Retama, J. Hernando, B. Lopez-Ruiz, A. Hartl, D. Steinmüller, M. Stutzmann, E. Lopez-Cabarcos and J. A. Garrido, *Langmuir*, 2006, **22**, 5837.
5 J. Hernando, T. Pourrostami, J. A. Garrido, O. A. Williams, D. M. Gruen, A. Kromka, D. Steinmüller and M. Stutzmann, *Diamond Relat. Mater.*, 2007, **16**, 138.
6 W. S. Yang, O. Auciello, J. E. Butler, W. Cai, J. A. Carlisle, J. Gerbi, D. M. Gruen, T. Knickerbocker, T. L. Lasseter, J. N. Russell, L. M. Smith and R. J. Hamers, *Nat. Mater.*, 2002, **1**, 253.
7 L. Marcon, M. Wang, Y. Coffinier, F. Le Normand, O. Melnyk, R. Boukherroub and S. Szunerits, *Langmuir*, 2010, **26**, 1075.
8 S. P. Cullen, I. C. Mandel and P. Gopalan, *Langmuir*, 2008, **24**, 13701.
9 T. Matrab, M. M. Chehimi, J. P. Boudou, F. Benedic, J. Wang, N. N. Naguib and J. A. Carlisle, *Diamond Relat. Mater.*, 2006, **15**, 639.
10 M. Steenackers, M. Jordan, A. Küller and M. Grunze, *Adv. Mater.*, 2009, **21**, 2921.
11 J. P. Deng, W. T. Yang and B. Rånby, *Macromol. Rapid Commun.*, 2001, **22**, 535.
12 M. Steenackers, S. Q. Lud, M. Niedermeier, P. Bruno, D. M. Gruen, P. Feulner, M. Stutzmann, J. A. Garrido and R. Jordan, *J. Am. Chem. Soc.*, 2007, **129**, 15655.
13 K. May, S. Dapprich, F. Furche, B. V. Unterreiner and R. Ahlrichs, *Phys. Chem. Chem. Phys.*, 2000, **2**, 5084.
14 N. Zhang, M. Steenackers, R. Luxenhofer and R. Jordan, *Macromolecules*, 2009, **42**, 5345.
15 N. Zhang, S. Huber, A. Schulz, R. Luxenhofer and R. Jordan, *Macromolecules*, 2009, **42**, 2215.
16 N. A. Hutter, A. Reitinger, N. Zhang, M. Steenackers, O. A. Williams, J. A. Garrido and R. Jordan, *Phys. Chem. Chem. Phys.*, 2010, **12**, 4360.
17 M. Patra and P. Linse, *Nano Lett.*, 2006, **6**, 133.
18 M. Steenackers, I. D. Sharp, K. Larsson, N. A. Hutter, M. Stutzmann and R. Jordan, *Chem. Mater.*, 2009, **22**, 272.
19 W. K. Lee, M. Patra, P. Linse and S. Zauscher, *Small*, 2007, **3**, 63.
20 (a) M. Steenackers, A. Küller, N. Ballav, M. Zharnikov, M. Grunze and R. Jordan, *Small*, 2007, **3**, 1764; (b) U. Schmelmer, A. Paul, A. Küller, M. Steenackers, A. Ulman, M. Grunze, A. Gölzhäuser and R. Jordan, *Small*, 2007, **3**, 459.
21 M. Steenackers, A. Küller, S. Stoycheva, M. Grunze and R. Jordan, *Langmuir*, 2009, **25**, 2225.
22 M. Ormö, A. B. Cubitt, K. Kallio, L. A. Gross, R. Y. Tsien and S. J. Remington, *Science*, 1996, **273**, 1392.
23 R. Heim, A. B. Cubitt and R. Y. Tsien, *Nature*, 1995, **373**, 663.
24 J. E. Gautrot, W. T. S. Huck, M. Welch and M. Ramstedt, *ACS Appl. Mater. Interfaces*, 2009, **2**, 193.
25 T. D. Craggs, *Chem. Soc. Rev.*, 2009, **38**, 2865.
26 W. W. Ward and S. H. Bokman, *Biochemistry*, 1982, **21**, 4535.
27 R. A. Dwek, *Chem. Rev.*, 1996, **96**, 683.
28 N. B. Holland, Y. X. Qiu, M. Ruegsegger and R. E. Marchant, *Nature*, 1998, **392**, 799.
29 F. C. Gaertner, R. Luxenhofer, B. Blechert, R. Jordan and M. Essler, *J. Control. Release*, 2007, **119**, 291.
30 A. Mero, G. Pasut, L. D. Via, M. W. M. Fijten, U. S. Schubert, R. Hoogenboom and F. M. Veronese, *J. Control. Release*, 2008, **125**, 87.
31 O. A. Williams, O. Douheret, M. Daenen, K. Haenen, E. Osawa and M. Takahashi, *Chem. Phys. Lett.*, 2007, **445**, 255.
32 W. Gajewski, O. A. Williams, P. Achatz, K. Haenen, E. Bustarret, M. Stutzmann and J. A. Garrido, *Phys. Rev. B: Condens. Matter Mater. Phys.*, 2009, **79**, 045206.